Author Manuscript

Author Manuscript

Author Manuscript

Author Manuscript

HHS Public Access

Author manuscript

Cell Rep. Author manuscript; available in PMC 2015 October 23.

Published in final edited form as:

Cell Rep. 2014 October 23; 9(2): 484–494. doi:10.1016/j.celrep.2014.09.010.

DOSAGE-DEPENDENT REGULATION OF PANCREATIC CANCER GROWTH AND ANGIOGENESIS BY HEDGEHOG SIGNALING

Esha Mathew[1], **Yaqing Zhang**[2], **Alexander M. Holtz**[1,3], **Kevin T. Kane**[2], **Jane Y. Song**[4], **Benjamin L. Allen**[1,4,*], and **Marina Pasca di Magliano**[1,2,4,*]

[1]Cellular and Molecular Biology Program, University of Michigan, Ann Arbor, MI, 48109, USA

[2]Department of Surgery, University of Michigan, Ann Arbor, MI, 48109, USA

[3]Medical Scientist Training Program, University of Michigan, Ann Arbor, MI, 48109, USA

[4]Department of Cell and Developmental Biology, University of Michigan, Ann Arbor, MI, 48109, USA

Summary

Pancreatic cancer, a hypovascular and highly desmoplastic cancer, is characterized by tumor expression of Hedgehog (HH) ligands which signal to fibroblasts in the surrounding stroma that in turn promote tumor survival and growth. However, the mechanisms and consequences of stromal HH pathway activation are not well understood. Here we show that the HH co-receptors GAS1, BOC, and CDON are expressed in cancer-associated fibroblasts. Deletion of two co-receptors (*Gas1* and *Boc*) in fibroblasts reduces HH-responsiveness. Strikingly, these fibroblasts promote greater tumor growth *in vivo* that correlates with increased tumor-associated vascularity. In contrast, deletion of all three co-receptors (*Gas1*, *Boc* and *Cdon*) results in the near complete abrogation of HH signaling and a corresponding failure to promote tumorigenesis and angiogenesis. Collectively, these data identify a novel role for HH-dosage in pancreatic cancer promotion and may explain the clinical failure of HH pathway blockade as a therapeutic approach in pancreatic cancer.

© 2014 The Authors. Published by Elsevier Inc.

*Corresponding authors: marinapa@umich.edu, Tel: 734-615-7424, Fax: 734-647-9654, benallen@umich.edu, Tel: 734-615-7512, Fax: 734-763-1166.

Publisher's Disclaimer: This is a PDF file of an unedited manuscript that has been accepted for publication. As a service to our customers we are providing this early version of the manuscript. The manuscript will undergo copyediting, typesetting, and review of the resulting proof before it is published in its final citable form. Please note that during the production process errors may be discovered which could affect the content, and all legal disclaimers that apply to the journal pertain.

Supplemental Information

Detailed experimental procedures and reagent information is provided in Supplemental Experimental Procedures.

Author Contributions

EM, BLA and MPdM conceived and designed the experiments. EM executed the experiments and collected the data. YZ, AMH, KK and JYS assisted with data collection and analysis. EM, BLA and MPdM wrote and edited the manuscript.

The authors declare they have no conflict of interest.

Author Manuscript Author Manuscript Author Manuscript Author Manuscript

Introduction

Pancreatic cancer, one of the deadliest human malignancies, is almost invariably associated with oncogenic mutations of *Kras* and the inappropriate activation of embryonic signaling pathways (Hruban et al., 2001; Jones et al., 2008). Pancreatic cancer is preceded by precursor lesions, the most common of which are Pancreatic Intraepithelial Neoplasias (PanINs) (Klimstra and Longnecker, 1994). Notably, tissue-specific expression of mutant *Kras* in mice recapitulates the step-wise progression of the human disease and constitutes a reasonable mouse model of pancreatic cancer (Hingorani et al., 2003).

Aberrant activation of Hedgehog (HH) signaling is observed in pancreatic cancer in both humans (Berman et al., 2003; Thayer et al., 2003) and mice (Hingorani et al., 2005). In pancreatic cancer, the HH pathway is proposed to act in a paracrine manner, where epithelial tumor cells secrete HH ligands that signal to cells of the tumor stroma (Yauch et al., 2008). HH signaling is activated by ligand binding to the twelve-pass transmembrane protein, Patched (PTCH1), which relieves an inhibitory effect on a second, GPCR-like protein, Smoothened (SMO) (Carpenter et al., 1998). De-repression of SMO results in a cascade of events that ultimately leads to the activation of GLI transcription factors and modulated target gene expression. HH pathway components such as *Ptch1* and *Gli1* are direct transcriptional targets, thus establishing a feedback loop that regulates the level of pathway activity (Agren et al., 2004; Dai et al., 1999).

In tumors classically associated with cell-autonomous activation of HH signaling, such as Basal cell carcinoma and Medulloblastoma, HH inhibition has emerged as a therapeutic strategy (Molckovsky and Siu, 2008; Rudin et al., 2009). Small molecule inhibitors that target SMO have been successfully developed to inhibit signaling and induce tumor regression (Rudin et al., 2009). HH inhibitors have also been applied to tumor types that rely on paracrine HH signaling (Yauch et al., 2008). While SMO inhibition in the clinic has met with initial success, the emergence of drug-resistant *Smo* mutations in tumors (Yauch et al., 2009) underscores the need for alternative approaches to restrict HH pathway function.

GAS1, BOC and CDON are cell surface-associated proteins that bind HH ligands and function as pathway activators (Allen et al., 2007; Martinelli and Fan, 2007; Tenzen et al., 2006; Zhang et al., 2006). During neural tube development, GAS1, BOC and CDON are required for HH signal transduction (Allen et al., 2011). However, despite their collective requirement during HH-dependent embryogenesis, the role of these proteins has not been explored in adult tissues and organs, and their potential contribution to disease, including cancer, is currently unknown.

Here, we investigated *Gas1*, *Boc* and *Cdon* expression and function in pancreatic cancer to determine whether they constitute potential novel therapeutic targets. We found that all three co-receptors were expressed in the adult pancreas and upregulated in pancreatic cancer stroma. We also observed that, similar to their role in embryogenesis, these co-receptors were required to mediate HH signal transduction in pancreatic fibroblasts. Counter to prevailing paradigms, while deletion of two co-receptors (*Gas1* and *Boc*) in pancreatic fibroblasts led to reduced HH-responsiveness, this resulted in increased tumor growth. In

Author Manuscript Author Manuscript Author Manuscript Author Manuscript

contrast, deletion of all three co-receptors (*Gas1*, *Boc* and *Cdon*) abrogated HH signaling and blocked tumor promotion. Notably, the tumor promoting effects of reduced HH signaling were due to increased angiogenesis mediated by the tumor stroma. These findings uncover a novel dosage-dependent role of HH signaling in the regulation of tumor angiogenesis in pancreatic cancer.

Results and Discussion

Gas1, *Boc*, and *Cdon* are expressed in fibroblasts and stellate cells in the normal adult and neoplastic pancreas

Given the requirement of the HH co-receptors GAS1, BOC and CDON in embryonic development (Allen et al., 2011), we sought to identify a role for these HH pathway components in adult tissue. To determine if *Gas1*, *Boc* and *Cdon* were expressed in the normal pancreas, during pancreatitis, and/or in the neoplastic pancreas, we harvested pancreata from adult *wildtype* or *Ptf1aCre;LSL-Kras*^{G12D} (KC) mice (Hingorani et al., 2003). KC pancreata were harvested three weeks following the induction of acute pancreatitis using the CCK agonist caerulein; this treatment synergizes with oncogenic Kras to drive tissue-wide PanIN formation and the accumulation of a fibroinflammatory stroma (Guerra et al., 2007; Morris et al., 2010). Wildtype pancreata were harvested from either untreated adult animals or from animals one day after caerulein treatment, at the peak of pancreatitis. Expression of all three co-receptors, as measured by RT-qPCR analysis, was barely detectable in control tissue (untreated adult pancreata), but was significantly increased in KC pancreata. In addition, we observed a significant increase in *Boc* expression and a subtle increase in *Gas1* and *Cdon* expression in the pancreatitis samples (Figure 1A).

To determine the cellular compartment in which these co-receptors are expressed, we crossed mice bearing reporter alleles of *Gas1* (*Gas1*$^{LacZ/+}$; (Martinelli and Fan, 2007) or *Boc* (*Boc*$^{PLAP/+}$; (Okada et al., 2006; Zhang et al., 2011) into the KC model of pancreatic cancer (Figure 1B). Pancreata were harvested from adult animals three weeks after inducing acute pancreatitis. Analysis of control pancreata revealed a perivascular and periductal expression pattern for *Gas1* and *Boc*, as well as in scattered cells throughout the parenchyma (Figure 1B). Strikingly, in KC tissues, *Gas1* and *Boc* expression expanded throughout the stroma surrounding PanIN lesions (Figure 1B).

To confirm that the RT-qPCR and reporter allele expression data correlated with increased co-receptor protein levels, we performed antibody detection of GAS1, BOC and CDON in pancreatic tissue (Figure S1). Consistent with our gene expression data, we detected limited stromal expression of GAS1, BOC and CDON in the normal pancreas, and increased coreceptor expression in the stroma surrounding PanIN lesions. (Figure S1A). These data suggest that GAS1, BOC and CDON are expressed in a population of stromal cells in the adult pancreas that expands greatly during PanIN formation.

To identify the specific cell type within the stroma expressing these co-receptors, we performed antibody staining of tissue from PanIN-bearing KC; *Gas1*$^{LacZ/+}$ pancreata (Figure 1C; Figure S1B). *Gas1*^{LacZ} expression was excluded from epithelial (E-cadherin+) and hematopoeitic (CD45+) cells (Figure 1C, white arrows). Similarly, β-galactosidase (β-

Author Manuscript Author Manuscript Author Manuscript Author Manuscript

gal) was not detected in endothelial cells lining the blood vessels. In contrast, we detected widespread co-expression of β-gal with smooth muscle actin (SMA), a marker of activated fibroblasts (Figure 1C, yellow arrows), throughout the stroma, except immediately surrounding blood vessels (Figure S1B). *Gas1* expression in fibroblasts was confirmed by co-staining with antibodies directed against β-gal and Vimentin, another fibroblast marker (Sugimoto et al., 2006). We also performed antibody staining of tissue from PanIN-bearing KC; $Boc^{PLAP/+}$ pancreata (Figure S1C). Antibody detection of alkaline phosphatase (AP) co-localized with SMA, suggesting that *Gas1* and *Boc* were co-expressed in a population of fibroblasts in the pancreas. In contrast, no co-localization of AP with either E-cadherin or CK19, both epithelial markers, was observed (Figure S1C). Thus, Boc expression was confined to the mesenchymal compartment. Finally, we performed RT-qPCR analysis of primary mouse pancreatic tumor cells, fibroblasts, and flow-sorted macrophages from the Pft1a-Cre;LSL-$Kras^{G12D}$;$p53^{R172H/+}$(KPC) (Hingorani et al., 2005) and iKras (Collins et al., 2012) pancreatic cancer models. We detected expression of Sonic HH ligand (*Shh*) only in the tumor cells (Figure S1D), whereas only fibroblasts expressed *Gas1* (Figure S1E).

Two alternative models could explain the increase in *Gas1, Cdon* and *Boc* expression in the neoplastic pancreas– increased expression on a per cell basis, or increased expression due to increased numbers of fibroblasts expressing these co-receptors. To distinguish between these two possibilities, we normalized the expression of the co-receptors to the mesenchymal marker *Vimentin*. Using this approach, we observed no change in *Gas1*, *Cdon* and *Boc* expression in the neoplastic pancreas compared to control (Figure S1F). Thus, the increase in co-receptor expression is caused by an increase in the number of co-receptor expressing cells within the tissue.

To determine whether our findings were relevant to human samples, we performed RT-qPCR on resected human pancreatic cancer samples and adjacent uninvolved pancreas. Upregulation of all three co-receptors was detected in the tumor samples (Figure S1G). To determine which compartment expressed the co-receptors, we obtained RNA from primary human tumor cells and primary human cancer associated fibroblasts (CAFs). We found elevated co-receptor expression in the CAF population, but not in the tumor cells (Figure S1H). As expected, *VIMENTIN* and *E-CADHERIN* were restricted to the CAF and tumor compartments respectively, thus confirming the identity of the samples (Figure S1I). These data suggest that upregulation of HH co-receptors is a phenomenon observed in human pancreatic cancer and recapitulated in mouse models of this disease.

Together, these data demonstrate that *Gas1*, *Boc*, and, *Cdon* are expressed in fibroblasts in both normal and PanIN-bearing pancreata and that their expression increases during pancreatic tumorigenesis as activated fibroblasts accumulate in the pancreas. Notably, this expression pattern resembles that observed for *Ptch1* in KC mice (Tian et al., 2009), thus placing these co-receptors in the same cell population previously reported to respond to HH signaling in pancreatic cancer.

GAS1 and BOC mediate HH-responsiveness in pancreatic fibroblasts

GAS1, BOC and CDON promote HH signaling in the developing neural tube in a ligand-dependent manner (Allen et al., 2011). To determine whether these co-receptors are required

Author Manuscript Author Manuscript Author Manuscript Author Manuscript

to transduce HH signals in fibroblasts, we generated wildtype and *Gas1*$^{-/-}$;*Boc*$^{-/-}$ MEFs and treated them with control or SHH conditioned medium. The cells were harvested 48 hours after treatment and analyzed for HH target gene expression (*Gli1* and *Ptch1*). We found significantly attenuated, although measurable levels of *Ptch1* and *Gli1* expression in *Gas1*$^{-/-}$;*Boc*$^{-/-}$ fibroblasts compared to wildtype cells (Figure 2A). Activation of HH signaling in fibroblasts has been reported to promote tumor growth in co-transplantation experiments (Yauch et al., 2008). Thus, we predicted that *Gas1*$^{-/-}$;*Boc*$^{-/-}$ fibroblasts would display reduced tumor-promoting ability compared to wildtype cells. To test this hypothesis, we co-injected the human pancreatic cancer cell lines Hs766T and MiaPaCa with either wildtype or *Gas1*$^{-/-}$;*Boc*$^{-/-}$ MEFs in immune compromised mice (Figure 2B). Surprisingly, tumor cells co-injected with *Gas1*$^{-/-}$;*Boc*$^{-/-}$ MEFs grew significantly larger than tumor cells injected alone or co-injected with wildtype fibroblasts (Figure 2C,D and Figure S2A). Analysis of these tumors revealed comparable epithelial histology for all experimental cohorts, including the accumulation of a collagen-rich stroma (Figure 2C, inset). However, blood vessel density was dramatically increased in tumors coinjected with *Gas1*$^{-/-}$;*Boc*$^{-/-}$ fibroblasts compared to tumor cells alone or co-injected with wildtype fibroblasts (Figure 2C,E).

To study this phenomenon in a more physiologically relevant system, we performed a similar experiment with primary human pancreatic cancer cells (1319; (Li et al., 2007; Zhang et al., 2013) and primary pancreatic fibroblasts isolated from either wildtype or *Gas1*$^{-/-}$;*Boc*$^{-/-}$ E18.5 mouse embryos (Figure 2F). Despite the perinatal lethality of *Gas1*$^{-/-}$;*Boc*$^{-/-}$ embryos (Allen et al., 2011), histological analysis of E18.5 pancreata revealed no gross abnormalities (data not shown). To assess HH-responsiveness, we treated wildtype and *Gas1*$^{-/-}$;*Boc*$^{-/-}$ pancreatic fibroblasts with control or SHH-conditioned media and extracted RNA 24 hours later. Similar to the MEF lines, SHH treatment induced robust expression of both *Gli1* and *Ptch1* in wildtype pancreatic fibroblasts, whereas this response was significantly attenuated in *Gas1*$^{-/-}$;*Boc*$^{-/-}$ pancreatic fibroblasts (Figure 2F). Thus, HH co-receptors are required for normal HH signaling in both MEFs and pancreatic fibroblasts.

We then co-injected 1319 cells alone or in combination with either genotype of pancreatic fibroblasts into mice. Notably, 1319 cells express *SHH* in culture at levels comparable to Hs766T cells (Figure S2B). Injection of 1319 cells alone formed subcutaneous tumors that were larger upon co-injection with wildtype fibroblasts, as expected (Figure 2H) (Yauch et al., 2008). However, co-injection with *Gas1*$^{-/-}$;*Boc*$^{-/-}$ pancreatic fibroblasts resulted in even larger tumors (Figure 2H). Tumor histology from each cohort was similar as assessed by H&E and Gomori staining, with a marked ductal morphology and abundant stroma, thus resembling the most common histology of human pancreatic cancer (Figure 2G) (Collisson et al., 2011). However, CD31 immunostaining revealed a dramatic increase in vasculature within tumors co-injected with *Gas1*$^{-/-}$;*Boc*$^{-/-}$ pancreatic fibroblasts (Figures 2G and 2I). The *Gas1*$^{-/-}$;*Boc*$^{-/-}$ fibroblasts were detected in close association with blood vessels, as determined by β-gal immunostaining (Figure 2G). Thus, stromal deletion of *Gas1* and *Boc* results in attenuated HH-responsiveness that paradoxically increases tumor growth. Given the heterogeneity of stromal fibroblasts (Sugimoto et al., 2006), these *Gas1* and *Boc*

Author Manuscript Author Manuscript Author Manuscript Author Manuscript

expressing fibroblasts may represent a subset of cells in which HH ligands inhibit an angiogenic response.

Dosage-dependent stromal HH signaling differentially promotes pancreatic tumor growth

Our data contrast with previous studies in which SMO blockade in the stroma inhibits pancreatic tumor growth (Olive et al., 2009; Yauch et al., 2008). Notably, despite the significantly reduced response to HH signaling in *Gas1*$^{-/-}$*;Boc*$^{-/-}$ fibroblasts, these cells are not completely refractory to HH pathway stimulation (Figures 2A and 2F). One possibility is that the level of HH pathway activation differentially affects pancreatic tumor growth. To understand the relationship between HH signaling dosage and tumor promotion, we generated *Gas1*$^{-/-}$ *Boc*$^{-/-}$; *Cdon*$^{-/-}$ MEFs. Of note, we could not use pancreatic fibroblasts as triple null embryos die at E9.5 (Allen et al., 2011) at the onset of pancreas development. *Gas1*$^{-/-}$*Boc*$^{-/-}$;*Cdon*$^{-/-}$ MEFs had nearly undetectable activation of HH target genes when exposed to SHH conditioned medium (Figure 3A). We co-transplanted 1319 tumor cells alone, or with three different cohorts of MEFs: wildtype, *Gas1*$^{-/-}$*Boc*$^{-/-}$ and *Gas1*$^{-/-}$*Boc*$^{-/-}$;*Cdon*$^{-/-}$ (Figure 3B). Again, wildtype MEFs promoted tumor growth compared to tumor cells alone, and *Gas1*$^{-/-}$*Boc*$^{-/-}$ MEFs promoted tumor growth further (Figure 3C). In contrast, tumors co-injected with *Gas1*$^{-/-}$;*Boc*$^{-/-}$;*Cdon*$^{-/-}$ MEFs were comparable both in growth rate and size at dissection to tumor cells alone (Figures 3C and 3D). These data are consistent with the reduced tumor-promoting ability of *Smo*$^{-/-}$ MEFs that are refractory to HH stimulation (Yauch et al., 2008). While cell death was similar in all experimental cohorts, we detected increased intratumoral proliferation in co-injections with tumor cells and *Gas1*$^{-/-}$*Boc*$^{-/-}$ MEFs; this effect was abrogated in co-injections with *Gas1*$^{-/-}$;*Boc*$^{-/-}$;*Cdon*$^{-/-}$ MEFs (Figure S3A). To verify that the co-injected MEFs persisted within the tumor at the time of analysis, we took advantage of lineage tracing provided by the expression of the β-gal reporter from the *Gas1* locus in these cells. By β-gal staining and quantitation we detected that both double and triple knock-out cells were present within the tumors (Figure 3E and Figure S3B).

Although tumor size varied between the different experimental groups, the histology was similar, with ductal structures surrounded by collagen rich stroma (Figure 3E). Notably, the level of *SHH* ligand, produced by the tumor cells (detected with human-specific primers and normalized to human *CYCLOPHILIN*) did not change among the different groups (Figure S3C). Genetic inactivation of *Shh* in multiple mouse models of pancreatic cancer resulted in variable reduction of stroma accumulation in different settings (Dai et al., 1999; Lee et al., 2014). To further investigate potential changes to the stroma in our model, we quantified the relative ratio of mesenchymal cells within the tumors (identified by immunostaining for Vimentin), and observed no measurable change (Figures S3A and S3D). Furthermore, RT-qPCR analysis for *Collagen I* revealed no difference among the different cohorts (Figure S3E), indicating no changes in fibrosis. The differences between the two models might derive from the different timing of HH pathway alteration. Interestingly, analysis of pre- and post-treatment biopsies of liver metastases in a recent clinical trial of the HH inhibitor GDC-0449 revealed only a mild reduction of fibrosis in half the patients, and no changes in fibrosis in the other half, consistent with our findings (Dr Diane Simeone, University of Michigan, *personal communication*).

Author Manuscript Author Manuscript Author Manuscript Author Manuscript

While the accumulation of fibroblasts within the stroma did not change, the number of blood vessels was significantly increased in tumors co-injected with *Gas1*$^{-/-}$*Boc*$^{-/-}$ MEFs but not in tumors co-injected with *Gas1*$^{-/-}$;*Boc*$^{-/-}$;*Cdon*$^{-/-}$ MEFs compared with control, as quantified by CD31 immunostaining (Figures 3E and 3F). A similar increase in vasculature was previously observed following genetic ablation of *Shh* or following drug-mediated inhibition of SMO, although the mechanism remained to be investigated (Dai et al., 1999; Lee et al., 2014; Olive et al., 2009). Thus, reduced HH response promotes tumor vascularity and growth, whereas complete HH pathway blockade fails to promote tumor growth (Figure 3G).

Reduced HH signaling promotes angiogenesis

To determine the mechanism by which reduced HH signaling promotes tumor growth and vascularity, we measured the expression of several angiogenic factors by RT-qPCR (Figures 4A and 4B). Along with VEGFa, the angiopoietins (ANGPT1 and ANGPT2) encompass a family of factors that act on the vascular endothelium (Augustin et al., 2009). In both *Gas1*$^{-/-}$ *Boc*$^{-/-}$ MEFs and pancreatic fibroblasts, *Angpt2* was upregulated compared to control pancreatic fibroblasts and MEFs respectively; in contrast, *Angpt2* expression in *Gas1*$^{-/-}$;*Boc*$^{-/-}$;*Cdon*$^{-/-}$ MEFs was comparable to wildtype MEFS (Figures 4A and 4B). The expression of other angiogenic factors varied between MEFs and pancreatic fibroblasts, although in all cases, reduced HH signaling resulted in increased expression of angiogenic factors, while the abrogation of HH signaling inhibited angiogenic gene expression (Figures 4A and 4B). For example, *Angpt1* expression was significantly upregulated in *Gas1*$^{-/-}$;*Boc*$^{-/-}$ pancreatic fibroblasts (Figure 4A), while *VEGFa*, previously described as a HH target in stromal perivascular cells (Chen et al., 2011) was upregulated in *Gas1*$^{-/-}$;*Boc*$^{-/-}$ MEFs (Figure 4B). The specific gene programs activated were not identical, possibly indicating distinct properties of fibroblasts of different origins.

To determine whether the change in expression of the angiogenic factors depended on ligand-mediated HH signaling, we treated wildtype or *Gas1*$^{-/-}$*Boc*$^{-/-}$ pancreatic fibroblasts with control conditioned medium or SHH conditioned medium. SHH treatment induced expression of *Vegfa* and *Angpt1*, while repressing expression of *Angpt2* (Figure S4A) consistent with previous publications (Lee et al., 2007; Zhang et al., 2011). The induction of *Vegfa* and overall expression levels were similar in *Gas1*$^{-/-}$*Boc*$^{-/-}$ pancreatic fibroblasts. In contrast, both *Angpt1* and *Angpt2* had higher basal expression levels in *Gas1*$^{-/-}$*Boc*$^{-/-}$ pancreatic fibroblasts, but the extent of relative induction or repression in response to SHH was reduced compared to wildtype fibroblasts, indicating that both ligand-dependent and ligand-independent mechanisms regulated the expression of these angiogenic factors (Figures S4A and S4B).

To further dissect the angiogenic properties of fibroblasts lacking *Gas1* and *Boc*, we used the chick chorioallantoic membrane (CAM) assay. *Gas1*$^{-/-}$;*Boc*$^{-/-}$ pancreatic fibroblasts and MEFs implanted alone atop the CAM induced the formation of more blood vessels than wildtype MEFs. Notably, this pro-angiogenic effect was not detected in *Gas1*$^{-/-}$;*Boc*$^{-/-}$;*Cdon*$^{-/-}$ MEFs (Figure S4C).

Author Manuscript Author Manuscript Author Manuscript Author Manuscript

We next co-implanted 1319 tumor cells with wildtype or *Gas1*$^{-/-}$;*Boc*$^{-/-}$ pancreatic fibroblasts. Wildtype fibroblasts promoted tumor growth in CAM assays, in agreement with our observations in the mouse (Figure 4C). Again, *Gas1*$^{-/-}$;*Boc*$^{-/-}$ pancreatic fibroblasts promoted the growth of even larger, more vascularized tumors (Figures 4C and 4D). Similar results were obtained using a primary mouse pancreatic cancer cell line (Zhang et al., 2013) derived from the KPC (Hingorani et al., 2005) pancreatic cancer model (Figure S4D).

We then tested *Gas1*$^{-/-}$;*Boc*$^{-/-}$;*Cdon*$^{-/-}$ MEFs in this assay and observed reduced tumor growth and vascularization (Figures 4E and 4F), indicating that tumor promotion and angiogenesis are specifically linked to the degree of HH-responsiveness. Similar to the subcutaneous tumor injections, *Gas1*$^{-/-}$;*Boc*$^{-/-}$;*Cdon*$^{-/-}$ fibroblasts did not impact tumor growth compared to tumor cells alone (Figure 4F).

Significance

The Hedgehog co-receptors *Gas1, Cdon* and *Boc* are required to mediate HH signaling during embryonic development (Allen et al., 2011), but their potential role in adult tissues and in disease remained largely unexplored. Here, we show that these co-receptors are expressed in pancreatic cancer and modulate the levels of HH-responsiveness in pancreatic fibroblasts. Despite initial expectations that fibroblasts with reduced HH-responsiveness would be impaired in their ability to support tumor growth, surprisingly, we found that these cells promoted tumor growth to a significantly greater extent than wildtype fibroblasts. Although HH pathway inhibition showed promise in mouse models of pancreatic cancer (Olive et al., 2009), clinical trials in humans were unsuccessful (Amakye et al., 2013). Treatment with HH inhibitors in human patients are likely to result in a strong reduction, but not complete inactivation, of HH signaling, since the drugs are continuously metabolized and excreted in between doses. Here we show that HH dosage is a key consideration in cancer treatment, where reduced levels of HH signaling evoke a potent angiogenic response. Thus, an angiogenic response might constitute a clinical readout of successful, but partial, HH blockade in vivo. While dosage-specific HH response has not been considered in cancer, developmental biology provides ample evidence of HH target genes activated at specific thresholds of signaling (for review, see (Jessell, 2000)). Further, although angiogenic blockade has not been used in pancreatic cancer due to its hypovascularity, our results raise the possibility that HH pathway blockade in pancreatic cancer may render tumors susceptible to anti-angiogenic therapy. A recent study indicates a possible benefit of this combination therapy on a mesenchymal subtype of pancreatic cancer in genetically engineered mice (Dai et al., 1999). Whether the failure of the recent HH inhibition trials in pancreatic cancer are due to an increase in angiogenesis should be investigated.

Another aspect of interest is the finding that MEFs and pancreatic fibroblasts have differences in HH-mediated gene regulation. The differences among fibroblasts populations in different organs are poorly understood, and might play an important role in cancer treatment, as fibroblasts at the metastatic sites might respond differently to treatment compared to fibroblasts at the primary site. HH signaling has been associated with pancreatic cancer metastasis (Feldmann et al., 2007), indicating the need for further studies

Author Manuscript Author Manuscript Author Manuscript Author Manuscript

aimed at characterizing HH response in fibroblasts derived from the pancreas and from common metastatic sites (such as liver and lung).

Experimental Procedures

Mice

Mice were housed in specific pathogen-free facilities of the University of Michigan Comprehensive Cancer Center. This study was approved by the University of Michigan University Committee on Use and Care of Animals (UCUCA) guidelines. Ptf1a-Cre mice (Kawaguchi et al., 2002) were intercrossed with LSL-Kras^{G12D} (Hingorani et al., 2003) to generate Ptf1a-Cre;LSL-Kras^{G12D} (KC) animals. KC mutant mice were further crossed with mice bearing reporter alleles *Gas1*$^{LacZ/+}$ (Martinelli and Fan, 2007) or *Boc*$^{AP/+}$ (Zhang et al., 2011) to generate KC;*Gas1*$^{LacZ/+}$ or KC;*Boc*$^{AP/+}$. Acute pancreatitis was induced by two 8-hourly series of intraperitoneal injections with caerulein (Sigma) at a concentration of 75ug/kg over a 48-hour period, as previously described (Morris et al., 2010).

Cell culture

Primary mouse pancreatic fibroblast lines were derived from E18.5 wildtype or *Gas1*$^{-/-}$;*Boc*$^{-/-}$ pancreata. Embryonic pancreas were minced via vigorous pipetting then immediately plated. MEFs were isolated and established using the methods of Todaro and Green (Todaro and Green, 1963). Samples were cultured in IMDM supplemented with 10% FBS and 1% penicillin/streptomycin (Gibco). For HH signaling assays, plated cells were serum-starved (IMDM supplemented with 0.5% serum) for 36h prior to addition of conditioned media, and samples collected at indicated timepoints.

Statistical Analysis

The data is expressed as the mean ± SEM. One-way ANOVA with a Tukey post-test and Student's t-tests were used to compare data. A p value <0.05 was considered statistically significant. Significance values indicated by asterisks are as follows: *p<0.05, **p < 0.01, ***p < 0.0005, ****p < 0.0001

Supplementary Material

Refer to Web version on PubMed Central for supplementary material.

Acknowledgements

We thank Drs Diane Simeone, Meghna Waghray, Lidong Wang and Ethan Abel (University of Michigan) for providing the 1319 tumors cells, providing human sample RNA, and for sharing unpublished data. We thank Dr Chandan Kumar (University of Michigan) for sharing his expertise on publicly available gene expression datasets. We also thank Dr Andrew Rhim and Dr Angelina Londono-Joshi (University of Michigan) for sharing unpublished data. We thank Dr Deb Gumucio for critical reading of the manuscript.

This project was supported by the University of Michigan Biological Scholar Program, the University of Michigan Comprehensive Cancer Center, NCI-1R01CA151588-01 to MPdM and 1R21CA167122-01 to BLA and MPdM. EM was supported by a University of Michigan Program in Cellular and Molecular Biology training grant (NIH T32 GM007315) and a University of Michigan Gastrointestinal Training Grant (NIH T32 DK094775). AMH was supported by a University of Michigan Program in Cellular and Molecular Biology training grant (NIH T32 GM007315) and an NIH predoctoral fellowship (1F31NS081806-01A1). BLA was supported by an American Heart Association Scientist Development Grant (11SDG6380000).

Author Manuscript Author Manuscript Author Manuscript Author Manuscript

References

Agren M, Kogerman P, Kleman MI, Wessling M, Toftgard R. Expression of the PTCH1 tumor suppressor gene is regulated by alternative promoters and a single functional Gli-binding site. Gene. 2004; 330:101–114. [PubMed: 15087129]

Allen BL, Song JY, Izzi L, Althaus IW, Kang JS, Charron F, Krauss RS, McMahon AP. Overlapping roles and collective requirement for the coreceptors GAS1, CDO, and BOC in SHH pathway function. Dev Cell. 2011; 20:775–787. [PubMed: 21664576]

Allen BL, Tenzen T, McMahon AP. The Hedgehog-binding proteins Gas1 and Cdo cooperate to positively regulate Shh signaling during mouse development. Genes Dev. 2007; 21:1244–1257. [PubMed: 17504941]

Amakye D, Jagani Z, Dorsch M. Unraveling the therapeutic potential of the Hedgehog pathway in cancer. Nat Med. 2013; 19:1410–1422. [PubMed: 24202394]

Augustin HG, Koh GY, Thurston G, Alitalo K. Control of vascular morphogenesis and homeostasis through the angiopoietin-Tie system. Nat Rev Mol Cell Biol. 2009; 10:165–177. [PubMed: 19234476]

Berman DM, Karhadkar SS, Maitra A, Montes De Oca R, Gerstenblith MR, Briggs K, Parker AR, Shimada Y, Eshleman JR, Watkins DN, et al. Widespread requirement for Hedgehog ligand stimulation in growth of digestive tract tumours. Nature. 2003; 425:846–851. [PubMed: 14520411]

Carpenter D, Stone DM, Brush J, Ryan A, Armanini M, Frantz G, Rosenthal A, de Sauvage FJ. Characterization of two patched receptors for the vertebrate hedgehog protein family. Proc Natl Acad Sci U S A. 1998; 95:13630–13634. [PubMed: 9811851]

Chen W, Tang T, Eastham-Anderson J, Dunlap D, Alicke B, Nannini M, Gould S, Yauch R, Modrusan Z, DuPree KJ, et al. Canonical hedgehog signaling augments tumor angiogenesis by induction of VEGF-A in stromal perivascular cells. Proc Natl Acad Sci U S A. 2011; 108:9589–9594. [PubMed: 21597001]

Collins MA, Bednar F, Zhang Y, Brisset JC, Galban S, Galban CJ, Rakshit S, Flannagan KS, Adsay NV, Pasca di Magliano M. Oncogenic Kras is required for both the initiation and maintenance of pancreatic cancer in mice. J Clin Invest. 2012; 122:639–653. [PubMed: 22232209]

Collisson EA, Sadanandam A, Olson P, Gibb WJ, Truitt M, Gu S, Cooc J, Weinkle J, Kim GE, Jakkula L, et al. Subtypes of pancreatic ductal adenocarcinoma and their differing responses to therapy. Nat Med. 2011; 17:500–503. [PubMed: 21460848]

Dai P, Akimaru H, Tanaka Y, Maekawa T, Nakafuku M, Ishii S. Sonic Hedgehog-induced activation of the Gli1 promoter is mediated by GLI3. J Biol Chem. 1999; 274:8143–8152. [PubMed: 10075717]

Feldmann G, Dhara S, Fendrich V, Bedja D, Beaty R, Mullendore M, Karikari C, Alvarez H, Iacobuzio-Donahue C, Jimeno A, et al. Blockade of hedgehog signaling inhibits pancreatic cancer invasion and metastases: a new paradigm for combination therapy in solid cancers. Cancer Res. 2007; 67:2187–2196. [PubMed: 17332349]

Guerra C, Schuhmacher AJ, Canamero M, Grippo PJ, Verdaguer L, Perez-Gallego L, Dubus P, Sandgren EP, Barbacid M. Chronic pancreatitis is essential for induction of pancreatic ductal adenocarcinoma by K-Ras oncogenes in adult mice. Cancer Cell. 2007; 11:291–302. [PubMed: 17349585]

Hingorani SR, Petricoin EF, Maitra A, Rajapakse V, King C, Jacobetz MA, Ross S, Conrads TP, Veenstra TD, Hitt BA, et al. Preinvasive and invasive ductal pancreatic cancer and its early detection in the mouse. Cancer Cell. 2003; 4:437–450. [PubMed: 14706336]

Hingorani SR, Wang L, Multani AS, Combs C, Deramaudt TB, Hruban RH, Rustgi AK, Chang S, Tuveson DA. Trp53R172H and KrasG12D cooperate to promote chromosomal instability and widely metastatic pancreatic ductal adenocarcinoma in mice. Cancer Cell. 2005; 7:469–483. [PubMed: 15894267]

Hruban RH, Adsay NV, Albores-Saavedra J, Compton C, Garrett ES, Goodman SN, Kern SE, Klimstra DS, Kloppel G, Longnecker DS, et al. Pancreatic intraepithelial neoplasia: a new nomenclature and classification system for pancreatic duct lesions. Am J Surg Pathol. 2001; 25:579–586. [PubMed: 11342768]

Author Manuscript Author Manuscript Author Manuscript Author Manuscript

Jessell TM. Neuronal specification in the spinal cord: inductive signals and transcriptional codes. Nat Rev Genet. 2000; 1:20–29. [PubMed: 11262869]

Jones S, Zhang X, Parsons DW, Lin JC, Leary RJ, Angenendt P, Mankoo P, Carter H, Kamiyama H, Jimeno A, et al. Core signaling pathways in human pancreatic cancers revealed by global genomic analyses. Science. 2008; 321:1801–1806. [PubMed: 18772397]

Klimstra DS, Longnecker DS. K-ras mutations in pancreatic ductal proliferative lesions. Am J Pathol. 1994; 145:1547–1550. [PubMed: 7992857]

Lee JJ, Perera RM, Wang H, Wu DC, Liu XS, Han S, Fitamant J, Jones PD, Ghanta KS, Kawano S, et al. Stromal response to Hedgehog signaling restrains pancreatic cancer progression. Proc Natl Acad Sci U S A. 2014

Lee SW, Moskowitz MA, Sims JR. Sonic hedgehog inversely regulates the expression of angiopoietin-1 and angiopoietin-2 in fibroblasts. Int J Mol Med. 2007; 19:445–451. [PubMed: 17273793]

Li C, Heidt DG, Dalerba P, Burant CF, Zhang L, Adsay V, Wicha M, Clarke MF, Simeone DM. Identification of pancreatic cancer stem cells. Cancer Res. 2007; 67:1030–1037. [PubMed: 17283135]

Martinelli DC, Fan CM. Gas1 extends the range of Hedgehog action by facilitating its signaling. Genes Dev. 2007; 21:1231–1243. [PubMed: 17504940]

Molckovsky A, Siu LL. First-in-class, first-in-human phase I results of targeted agents: highlights of the 2008 American society of clinical oncology meeting. J Hematol Oncol. 2008; 1:20. [PubMed: 18959794]

Morris, JPt; Cano, DA.; Sekine, S.; Wang, SC.; Hebrok, M. Beta-catenin blocks Kras-dependent reprogramming of acini into pancreatic cancer precursor lesions in mice. J Clin Invest. 2010; 120:508–520. [PubMed: 20071774]

Olive KP, Jacobetz MA, Davidson CJ, Gopinathan A, McIntyre D, Honess D, Madhu B, Goldgraben MA, Caldwell ME, Allard D, et al. Inhibition of Hedgehog signaling enhances delivery of chemotherapy in a mouse model of pancreatic cancer. Science. 2009; 324:1457–1461. [PubMed: 19460966]

Rudin CM, Hann CL, Laterra J, Yauch RL, Callahan CA, Fu L, Holcomb T, Stinson J, Gould SE, Coleman B, et al. Treatment of medulloblastoma with hedgehog pathway inhibitor GDC-449. N Engl J Med. 2009; 361:1173–1178. [PubMed: 19726761]

Sugimoto H, Mundel TM, Kieran MW, Kalluri R. Identification of fibroblast heterogeneity in the tumor microenvironment. Cancer Biol Ther. 2006; 5:1640–1646. [PubMed: 17106243]

Tenzen T, Allen BL, Cole F, Kang JS, Krauss RS, McMahon AP. The cell surface membrane proteins Cdo and Boc are components and targets of the Hedgehog signaling pathway and feedback network in mice. Dev Cell. 2006; 10:647–656. [PubMed: 16647304]

Thayer SP, di Magliano MP, Heiser PW, Nielsen CM, Roberts DJ, Lauwers GY, Qi YP, Gysin S, Fernandez-del Castillo C, Yajnik V, et al. Hedgehog is an early and late mediator of pancreatic cancer tumorigenesis. Nature. 2003; 425:851–856. [PubMed: 14520413]

Tian H, Callahan CA, DuPree KJ, Darbonne WC, Ahn CP, Scales SJ, de Sauvage FJ. Hedgehog signaling is restricted to the stromal compartment during pancreatic carcinogenesis. Proc Natl Acad Sci U S A. 2009; 106:4254–4259. [PubMed: 19246386]

Todaro GJ, Green H. Quantitative studies of the growth of mouse embryo cells in culture and their development into established lines. J Cell Biol. 1963; 17:299–313. [PubMed: 13985244]

Yauch RL, Dijkgraaf GJ, Alicke B, Januario T, Ahn CP, Holcomb T, Pujara K, Stinson J, Callahan CA, Tang T, et al. Smoothened mutation confers resistance to a Hedgehog pathway inhibitor in medulloblastoma. Science. 2009; 326:572–574. [PubMed: 19726788]

Yauch RL, Gould SE, Scales SJ, Tang T, Tian H, Ahn CP, Marshall D, Fu L, Januario T, Kallop D, et al. A paracrine requirement for hedgehog signalling in cancer. Nature. 2008; 455:406–410. [PubMed: 18754008]

Zhang W, Hong M, Bae GU, Kang JS, Krauss RS. Boc modifies the holoprosencephaly spectrum of Cdo mutant mice. Dis Model Mech. 2011; 4:368–380. [PubMed: 21183473]

Author Manuscript Author Manuscript Author Manuscript Author Manuscript

Zhang W, Kang JS, Cole F, Yi MJ, Krauss RS. Cdo functions at multiple points in the Sonic Hedgehog pathway, and Cdo-deficient mice accurately model human holoprosencephaly. Dev Cell. 2006; 10:657–665. [PubMed: 16647303]

Zhang Y, Morris JPt, Yan W, Schofield HK, Gurney A, Simeone DM, Millar SE, Hoey T, Hebrok M, Pasca di Magliano M. Canonical wnt signaling is required for pancreatic carcinogenesis. Cancer Res. 2013; 73:4909–4922. [PubMed: 23761328]

Author Manuscript Author Manuscript Author Manuscript Author Manuscript

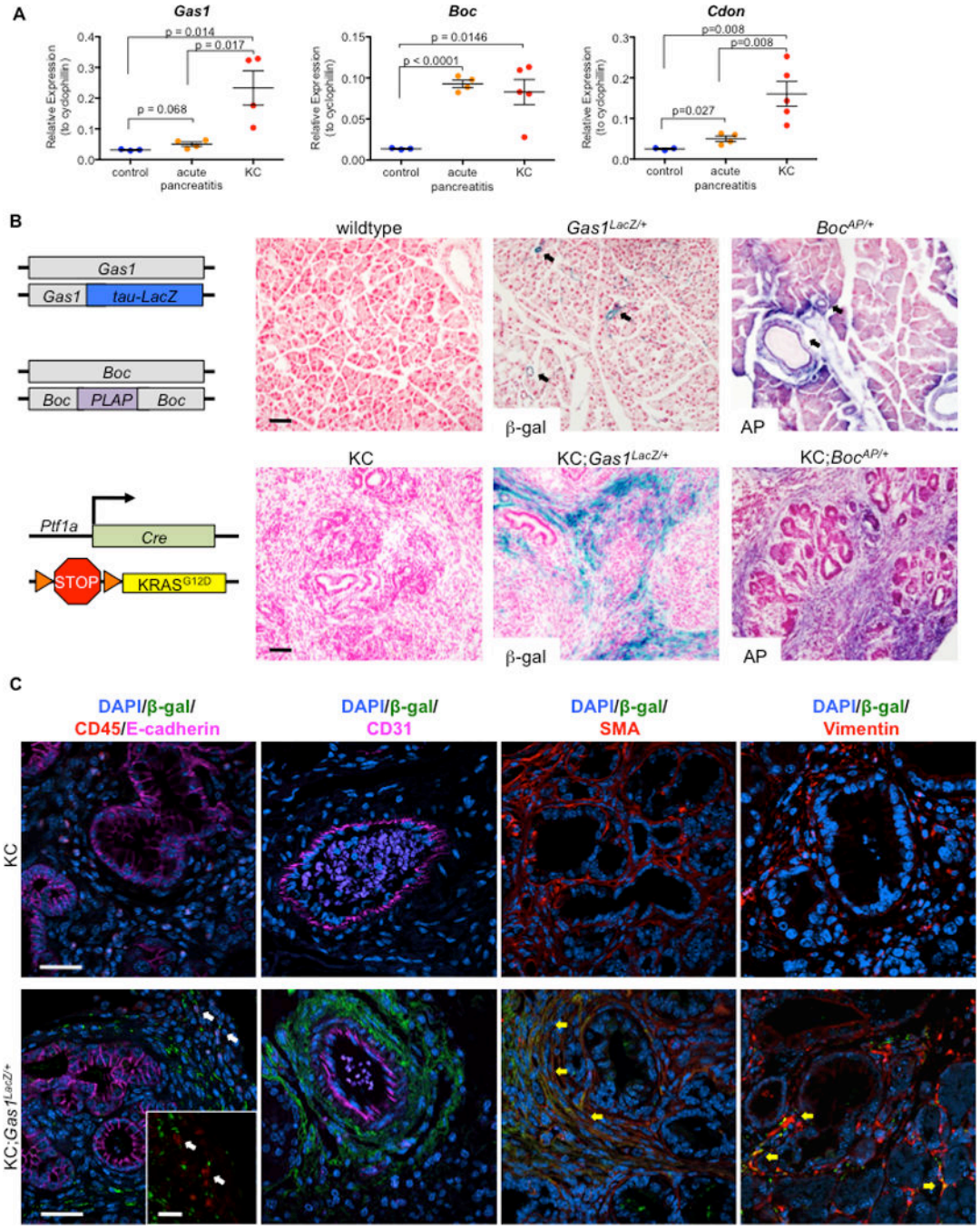

Figure 1. *Gas1*, *Boc*, and *Cdon* are expressed in the normal and neoplastic pancreas

RT-qPCR analysis for (A) *Gas1*, *Boc*, and *Cdon* in control (n=3), acute pancreatitis (n=4), and KC pancreata (n=5). (B) Schematic of *Gas1* and *Boc* reporter strains and KC model (left panels).Beta-galactosidase (β-gal) and Alkaline Phosphatase (AP) staining for *Gas1* and *Boc* reporter expression in normal and neoplastic pancreata (right panels). Scale bars, 50μm. (C) Antibody detection of β-gal (green) and CD45/E-cadherin (red/magenta), CD31 (magenta), SMA (red), and Vimentin (red) in KC and KC;$Gas1^{LacZ/+}$ PanIN lesions. DAPI (blue) marks nuclei. White arrows (left panel) indicate separate β-gal and CD45 expression; yellow

arrows (right panels) indicate co-expression of β-gal with SMA and Vimentin. Scale bar, 20μm.

Author Manuscript Author Manuscript Author Manuscript Author Manuscript

Author Manuscript
Author Manuscript
Author Manuscript
Author Manuscript

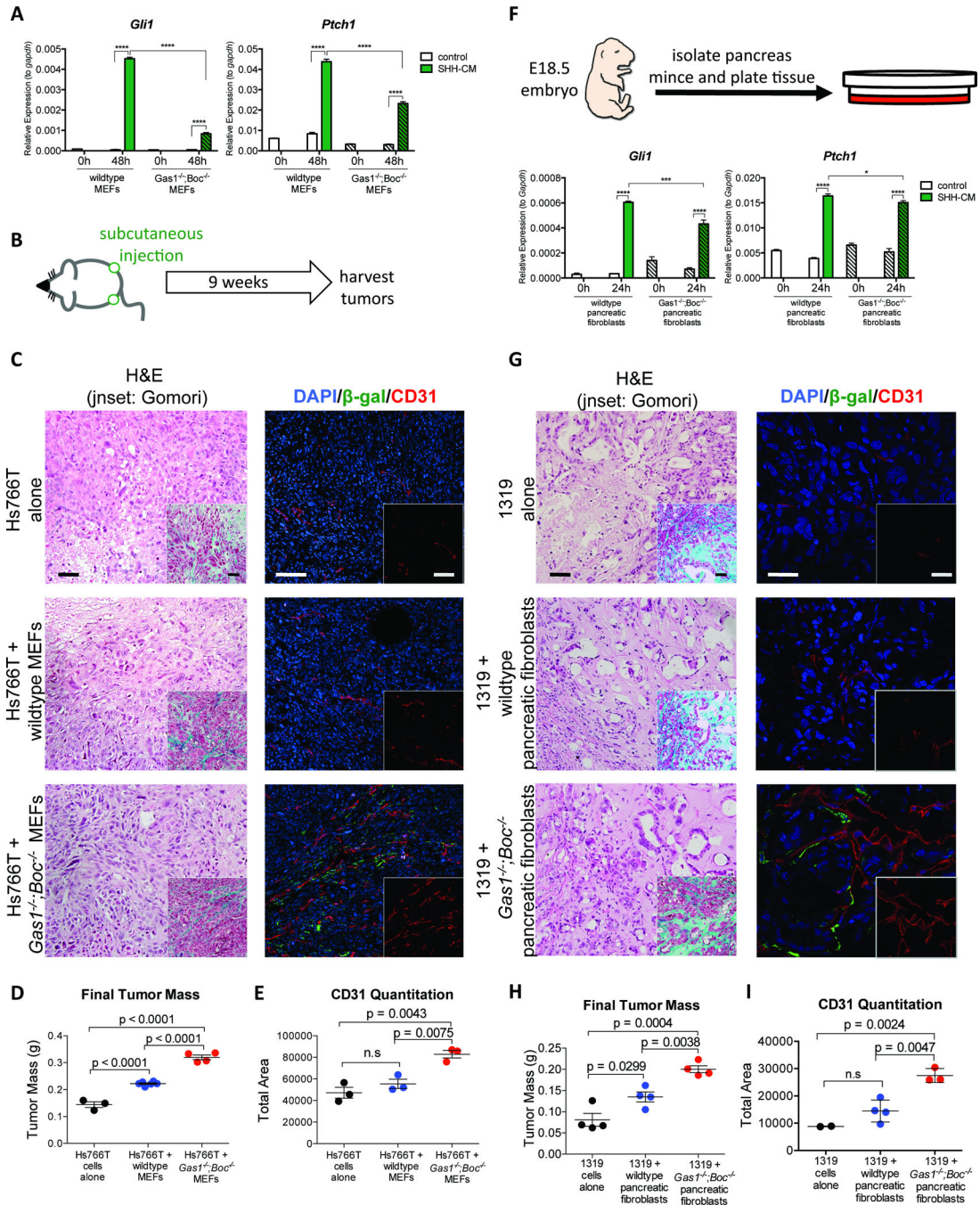

Figure 2. Stromal deletion of *Gas1* and *Boc* impairs HH-responsiveness, but promotes tumor growth

(A) RT-qPCR analysis of *Gli1* and *Ptch1* in MEFs. (B) Schematic of subcutaneous tumor injection experiment. (C) Histopathological analysis of tumors following co-injection of Hs766T cells with MEFs. Scale bar, 50μm, inset scale bar 50μm. H&E staining (left panels) and Gomori trichrome (inset, left panels). Antibody detection of β-gal (green) and CD31 (red; right panels). DAPI (blue) marks nuclei. Scale bar 50μm, inset scale bar 50μm. (D) Quantitation of final tumor size. (E) Quantitation of CD31 staining. (F) Schematic of

pancreatic fibroblast isolation. RTqPCR analysis of *Gli1* and *Ptch1*. (G) Histopathological analysis of tumors following co-injection of 1319 cells with pancreatic fibroblasts. Scale bar, 20μm, inset scale bar, 20μm. Antibody detection of β-gal (green) and CD31 (red; right panels). DAPI (blue) marks nuclei. Scale bar, 20μm, inset scale bar 20μm. (H) Quantitation of final tumor size and (I) CD31 staining.

Author Manuscript Author Manuscript Author Manuscript Author Manuscript

Author Manuscript Author Manuscript Author Manuscript Author Manuscript

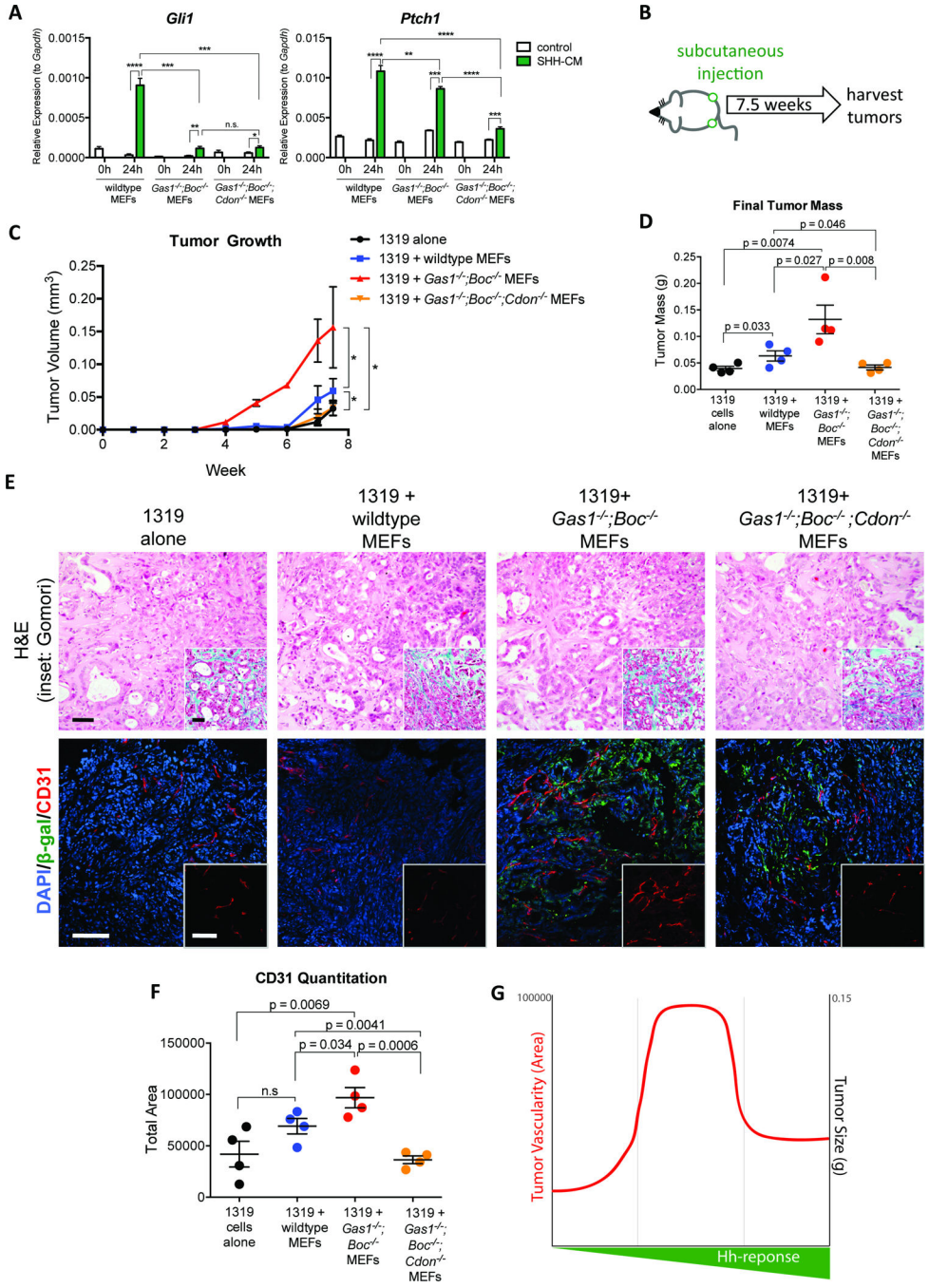

Figure 3. Dosage-dependant HH signaling differentially promotes pancreatic tumor growth

(A) RT-qPCR analysis for *Gli1* and *Ptch1* in MEFs. (B) Schematic of subcutaneous tumor injection experiment. (C) Growth curve for subcutaneous tumors. (D) Quantitation of final tumor size. (E) Histopathological analysis of tumors following co-injection of 1319 cells with MEFs. Scale bar, 50μm, inset scale bar 50μm. H&E staining (top panels) and Gomori trichrome (inset, top panels). Antibody detection of β-gal (green) and CD31 (red; bottom panels). DAPI (blue) marks nuclei. Scale bar 50μm, inset scale bar 50μm. (F) Quantitation of CD31 staining. (G) Comparison of tumor size and vascularity between fibroblast lines.

Author Manuscript Author Manuscript Author Manuscript Author Manuscript

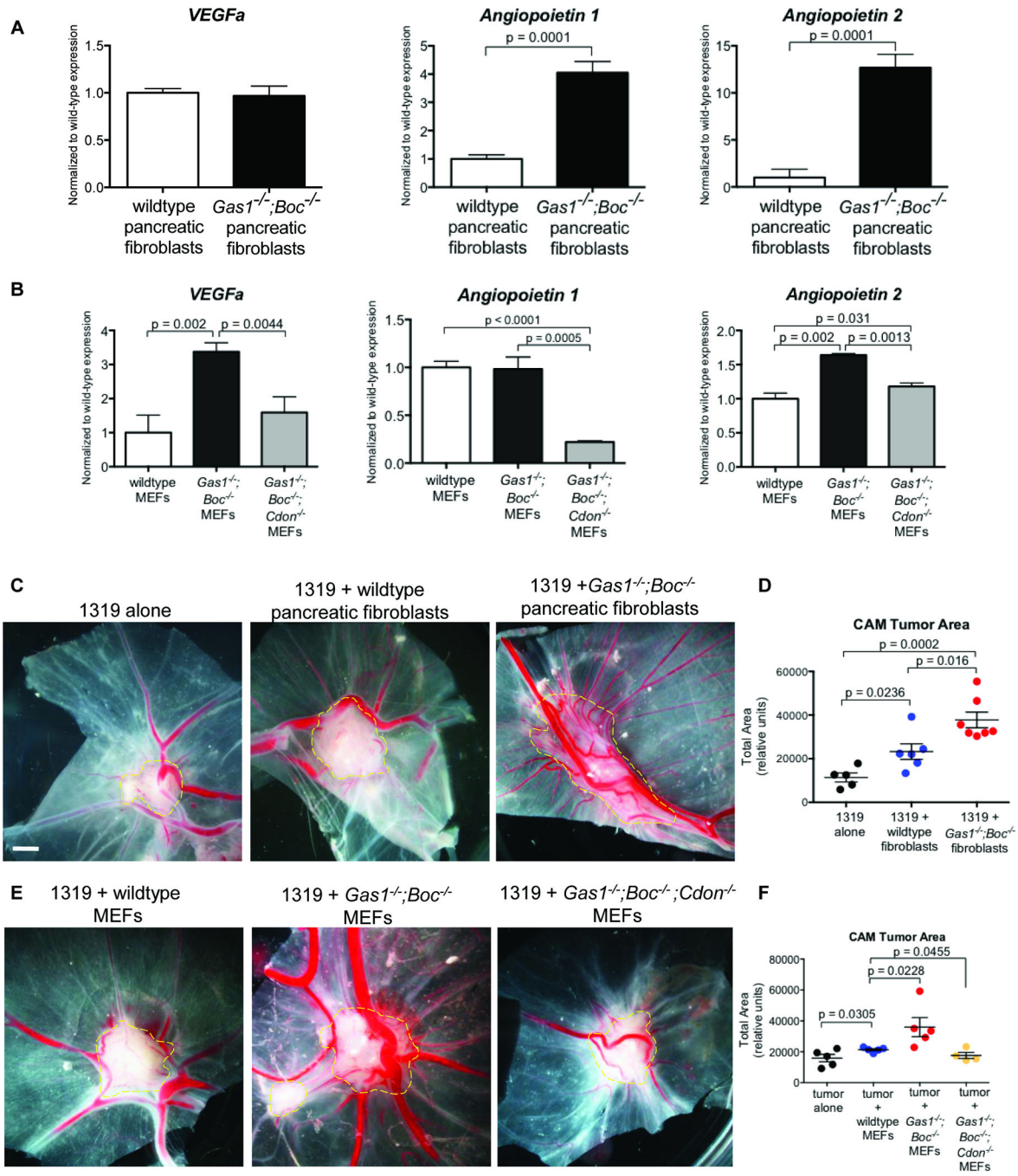

Figure 4. Angiogenesis regulation by fibroblasts in response to modulation of Hedgehog signaling

A) RT-qPCR analysis of *Vegfa*, *Anpgt1*, and *Anpgt2* in pancreatic fibroblasts and (B) in MEFs. (C) Chicken CAM assay with 1319 cells and pancreatic fibroblasts. (D) Quantitation of CAM tumor area. (E) Chicken CAM assay with 1319 cells and MEFs. (F) Quantitation of CAM tumor area. Scale bar, 2mm.